Supporting Information

Table S1. Effect of 18 different compounds on AP-1 or NF- *κ*B activity.

ID	Structure	NF-*κ*B activity	AP-1 activity
648	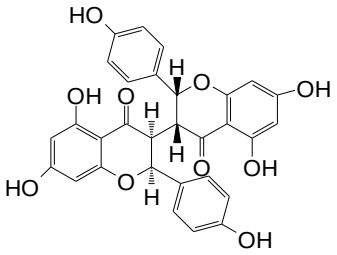	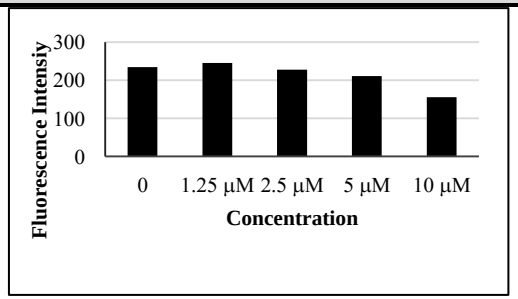	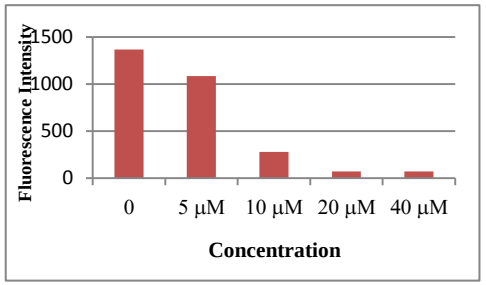
831	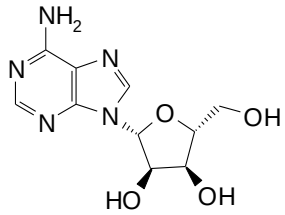	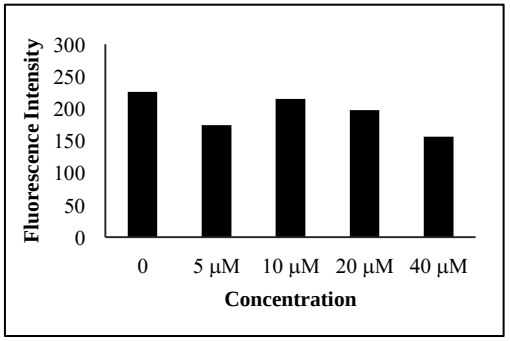	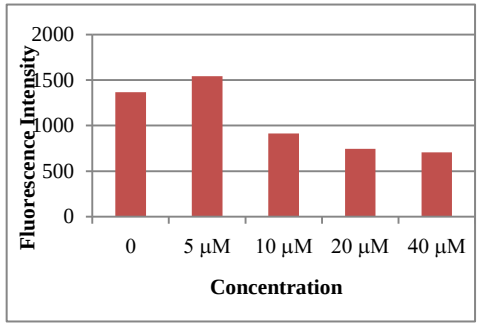

1326	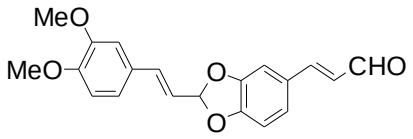	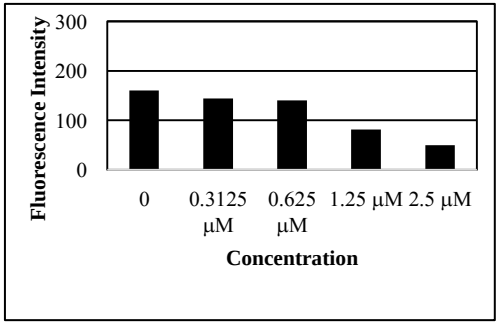	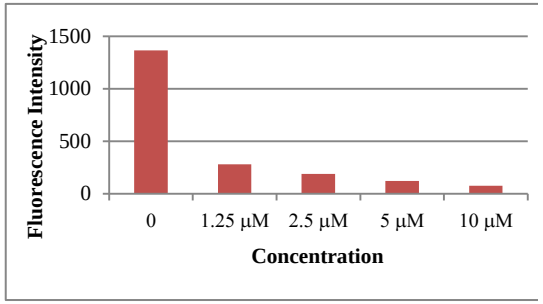
1337	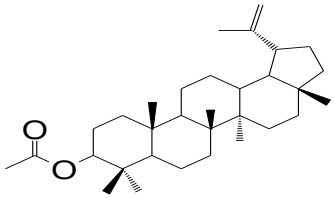	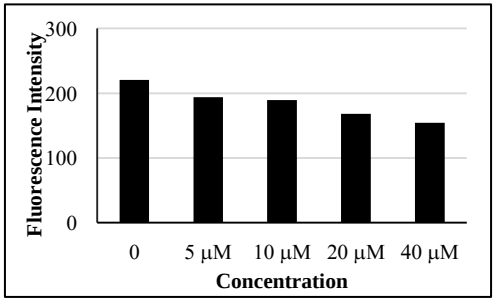	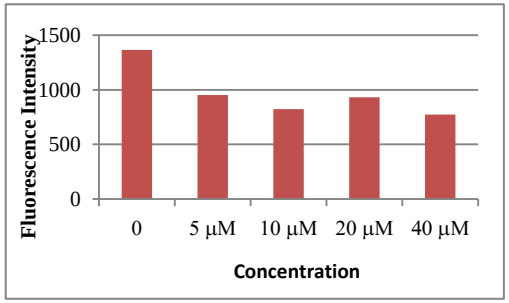
586	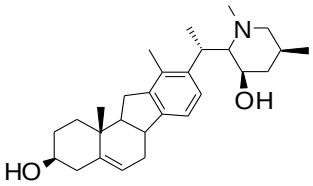	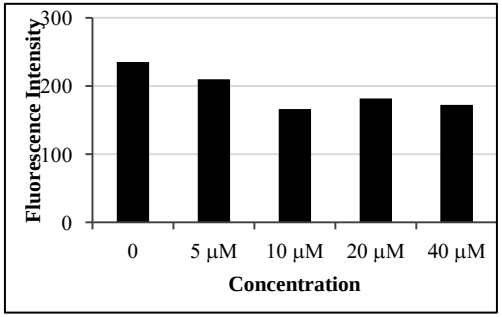	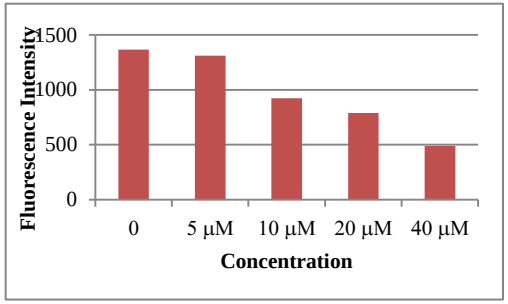

1125	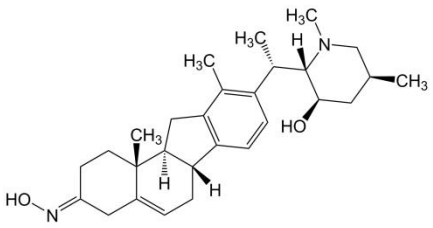	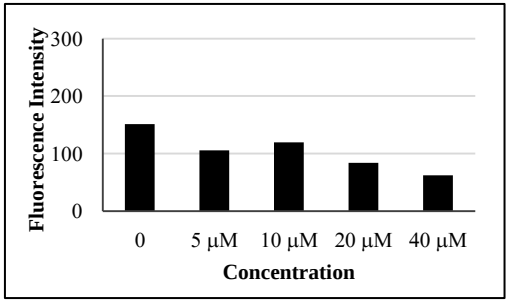	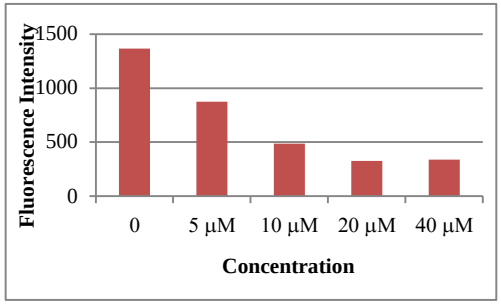
1126	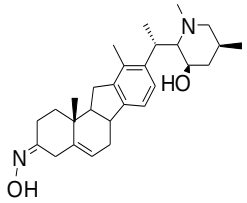	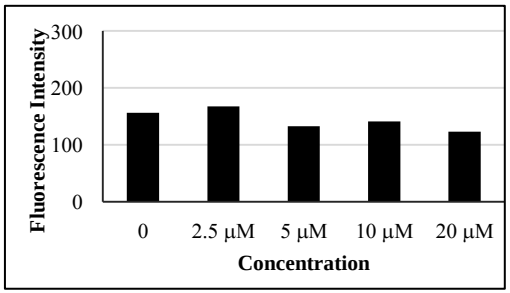	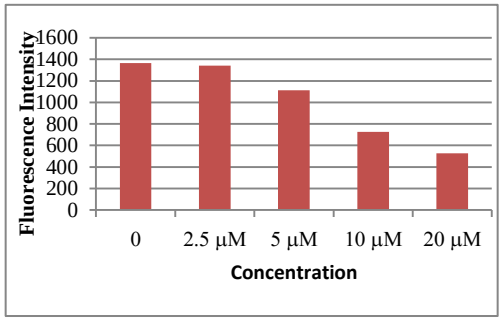
1134	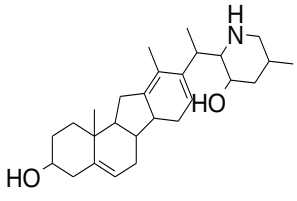	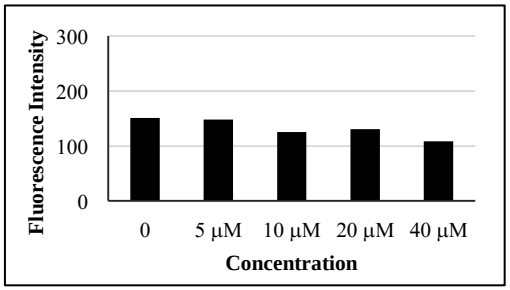	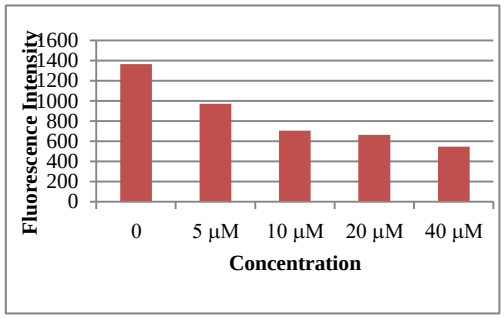

1423	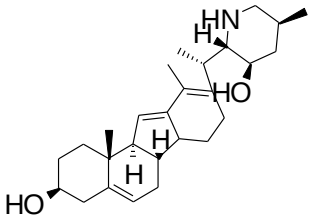	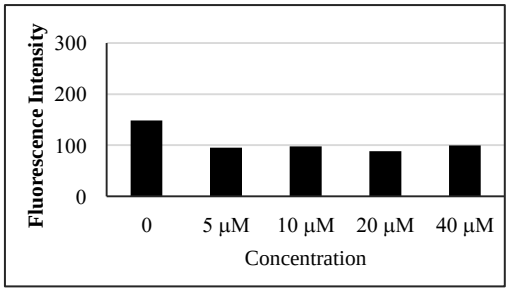	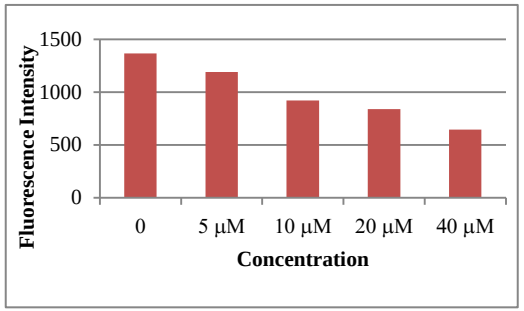
1451	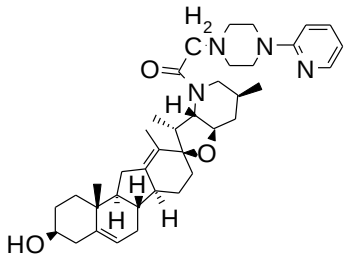	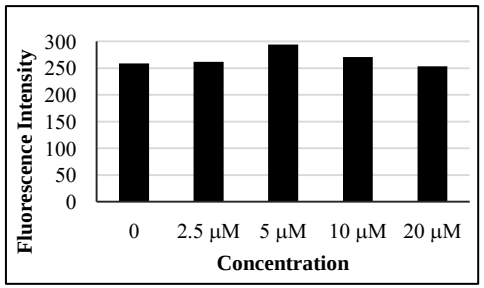	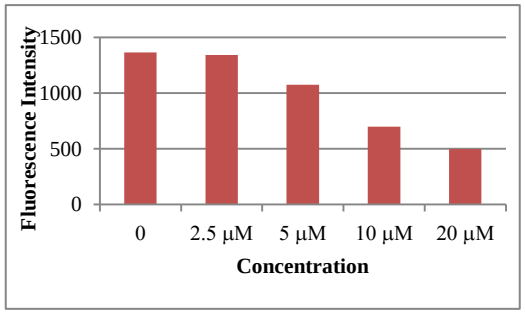
1460	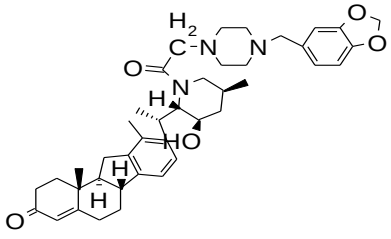	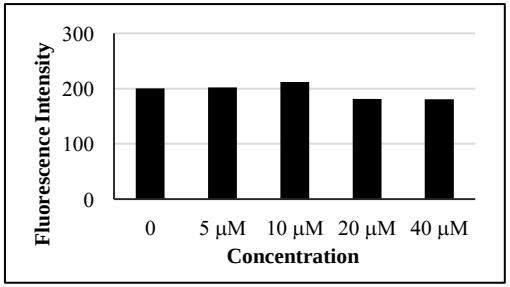	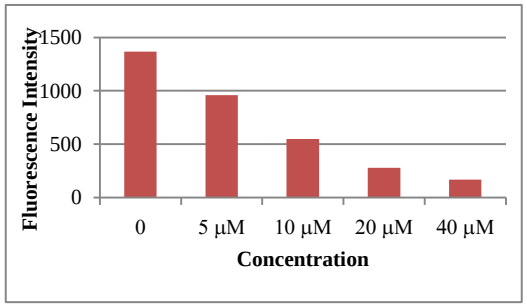

1504	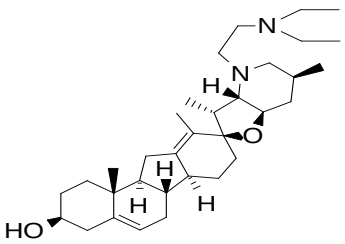	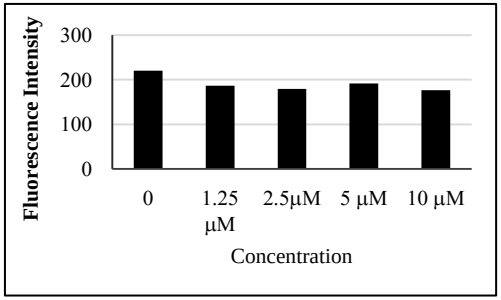	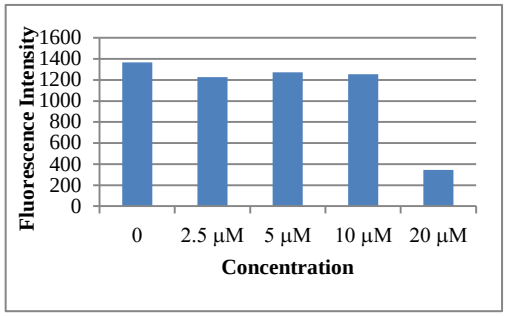
1512	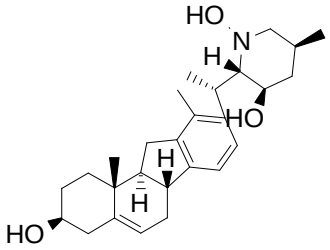	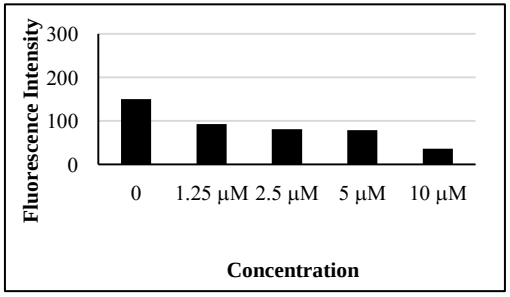	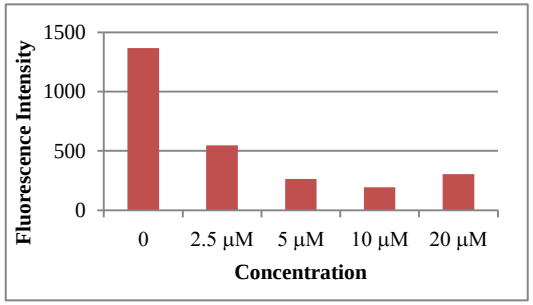
1037	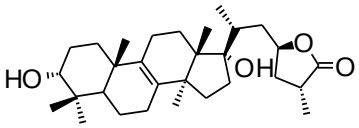	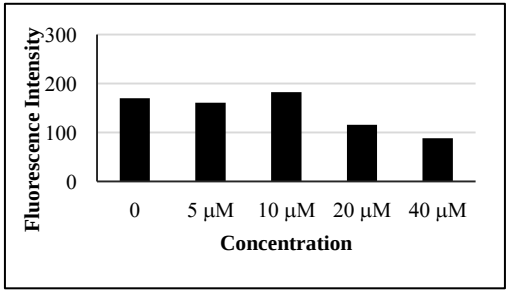	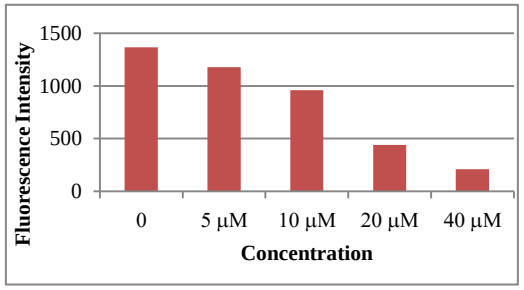

1529

(Veratramine)

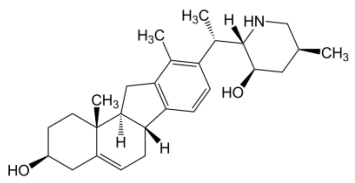

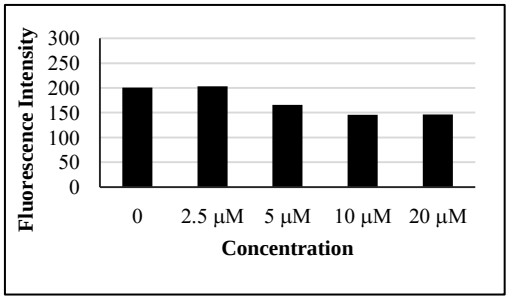

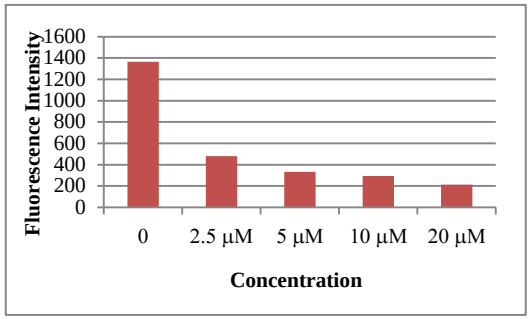

1530

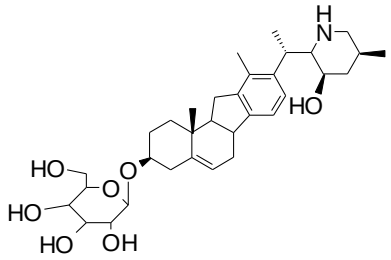

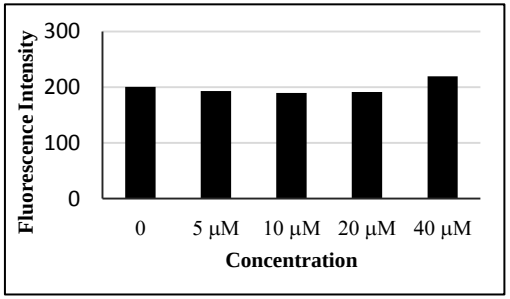

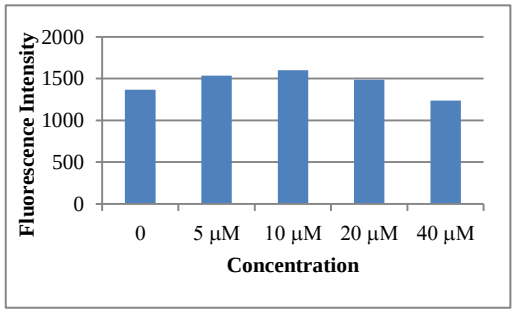

1474

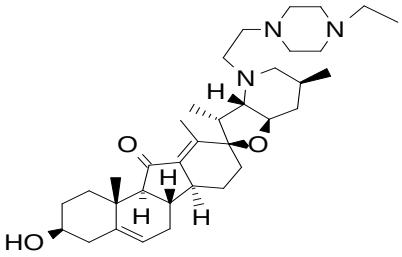

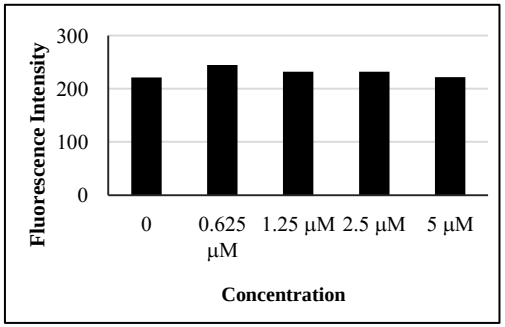

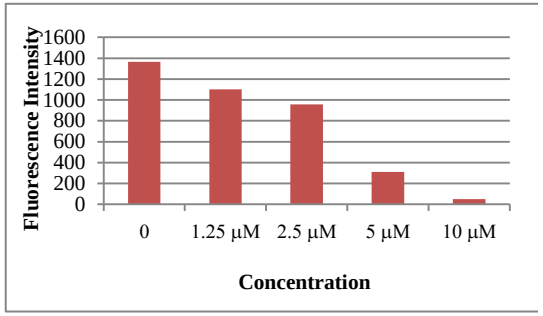

1517	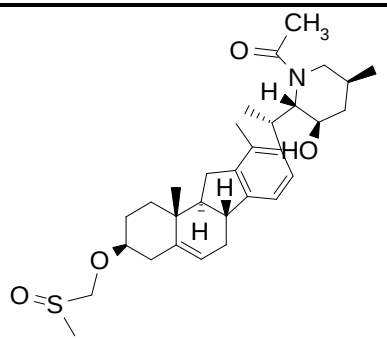	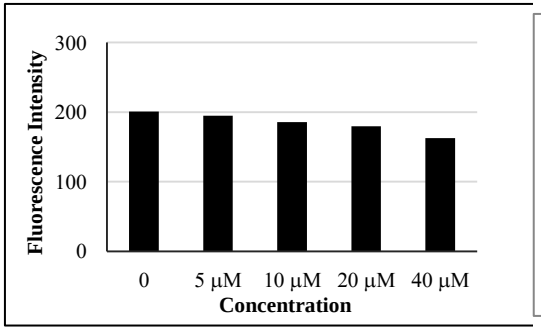	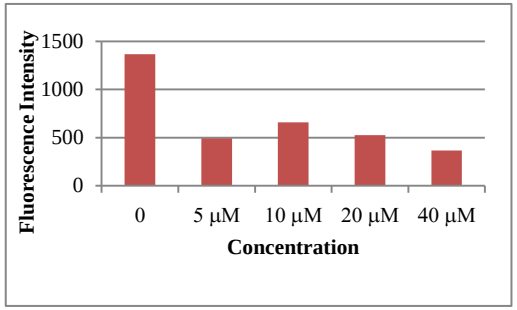

[a]Bioactivity data was not determined.

Table S2. Log2 fold changes in MAPK gene expression after treatment with veratramine or its analogue compounds 1125 or 1126.

Gene	Protein	Compound		
		1125	**1126**	**1529**
Mapk1	ERK2	0.205009	0.15988	0.022198
Mapk10	JNK3	N.A.[a]	NA	NA
Mapk11	P38b	-1.09863	-0.45989	-0.03327
Mapk12	p38r	0.158206	0.004317	-0.41042
Mapk13	p38s	N.A.	-0.26227	NA
Mapk14	p38a	0.503937	-0.16601	-0.05641
Mapk8	JNK1	-0.14252	9.48E-05	0.014034
Mapk9	JNk2	0.192236	0.430562	-0.25418
Mapk3	ERK1	-0.21661	-0.0048	0.28699

[a]Data not available

Figure S1. Gene set enrichment analysis (GSEA) confirms repression of downstream genes of AP1, but upregulation of upstream genes of AP1. Microarray data were analyzed using GSEA software to judge the modulation of AP-1 pathway genes by veratramine (1529), and the other two analogues (1125 and 1126). (a) In the enrichment plot, genes are ranked by signal/noise ratio according to their differential expression between the compound treated (10 μM 1529, 20μM 1125 or 1126) and control (treated with DMSO) mouse epidermal JB6 cell lines (three samples for each). Genes related AP-1 are ranked with vertical bars and the enrichment score is show in green. (b) Relative expression of AP-1 related genes in compound treated and control cell lines.

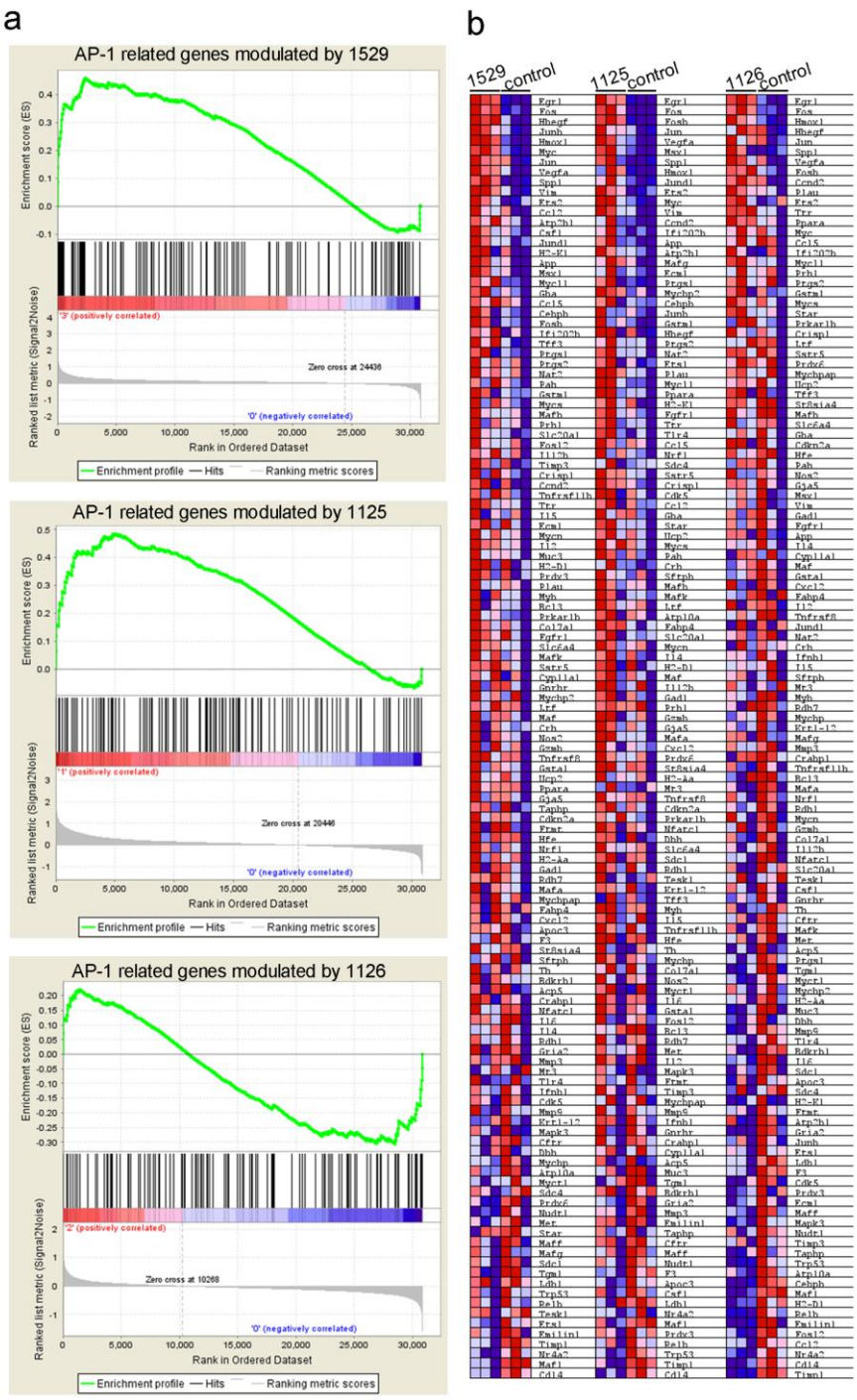

Brief description of *i*DNABinder

*i*DNABinder is an in-house specific molecular docking tool for DNA-ligand docking, whose scoring function comprises DNA-specific knowledge-based and force field-based scoring functions. The knowledge-based scoring function is defined as the sum of all weighted DNA-ligand atom pair potentials $A_{ij}(r)$ at a distance r within the given distance $r_{\text{cut-off}}$ (8.0 Å) as shown in equation 1,

$$U = \sum_{i}^{lig} \sum_{j}^{rec} A_{ij}(r) \qquad r \le r_{\text{cut-off}} \tag{1}$$

where $A_{ij}(r)$ is the atom-pair potential terms between ligand atom i and DNA atom j, which is obtained on the basis of the conventional inverse Boltzmann relation as shown in equation 2,

$$A_{ij}(r) = -k_B T \ln[f^{i}_{vol\_corr}(r) \rho^{ij}_{seg}(r) / \rho^{ij}_{bulk}(r)] \tag{2}$$

where T is the absolute temperature, k_B is the Boltzmann constant, $f^{i}_{\text{vol\_corr}}(r)$ is the ligand volume correction factor, $\rho^{ij}_{seg}(r)$ is the number density of atom pair (i, j) that occurs in a spherical shell between r and $r+\Delta r$, and $\rho^{ij}_{bulk}(r)$ is the number density of atom pair (i, j) that occurs in a reference sphere with radius R. In this study, we set R = 12.0 Å and Δr = 0.2 Å. Detailed calculations for $\rho^{ij}_{seg}(r)$ and $\rho^{ij}_{bulk}(r)$ are similar as that reported in our previous work for developing KScore(1) and MpSDock$_{Zn}$(2).

The force-field scoring function, including non-bonded Van der Waals interaction $E^{\text{VdW}}_{ik,MMFF94}$ and electrostatic interaction $E^{es}_{ik,MMFF94}$ (equation 3), is used to optimize the binding conformation of ligand, which is developed based on the MMFF94 force field(3).

$$E_{\text{lig}} = \sum_{i}^{lig} \sum_{k,i\neq k}^{lig} E^{\text{VdW}}_{ik,\text{MMFF94}}(r) + \sum_{i}^{lig} \sum_{k,i\neq k}^{lig} E^{es}_{ik,\text{MMFF94}}(r) \tag{3}$$

Given the different units between the knowledge-based and force field based scoring functions, the two scoring functions are designed as independent objective functions, which makes the docking process become a balanced optimization with a multi-objective optimization algorithm (nonsorting genetic algorithm II [NSGA II](4)).

References

1. Zhao, X., Liu, X., Wang, Y., Chen, Z., Kang, L., Zhang, H., Luo, X., Zhu, W., Chen, K., Li, H. et al. (2008) An Improved PMF Scoring Function for Universally Predicting the Interactions of a Ligand with Protein, DNA, and RNA. J. Chem. Infor. Model., 48, 1438-1447.

2. Bai, F., Liao, S., Gu, J., Jiang, H., Wang, X. and Li, H. (2015) An Accurate Metalloprotein-Specific Scoring Function and Molecular Docking Program Devised by a Dynamic Sampling and Iteration Optimization Strategy. J.Chem. Infor. Model., 55, 833-847.

3. Halgren, T.A. (1996) Merck molecular force field. I. Basis, form, scope, parameterization, and performance of MMFF94. J. Comput. Chem., 17, 490-519.

4. Deb, K., Pratap, A., Agarwal, S. and Meyarivan, T. (2002) A fast and elitist multiobjective genetic algorithm: NSGA-II. IEEE Trans. Evolut. Comput., 6, 182-197.